

1995

NASA/ASEE SUMMER FACULTY FELLOWSHIP PROGRAM

**MARSHALL SPACE FLIGHT CENTER
THE UNIVERSITY OF ALABAMA IN HUNTSVILLE**

TRIANGULATION METHODS FOR AUTOMATED DOCKING

Prepared by: John W. Bales, Ph. D.

Academic Rank: Associate Professor

**Institution and Department: Tuskegee University
Department of Mathematics**

NASA/MSFC:

**Directorate: Science and Engineering
Laboratory: Astrionics
Division: Avionics Simulation
Branch: Orbital Systems and Robotics**

MSFC Colleague: Fred Roe, Jr.

Introduction

An automated docking system must have a reliable method for determining range and

must also provide accurate information on the rates of change of range to and orientation of the passive vehicle. The method must be accurate within required tolerances and capable of operating in real time.

The method being developed at Marshall Space Flight Center employs a single TV camera, a laser illumination system and a target consisting, in its minimal configuration, of three retro-reflectors. Two of the retro-reflectors are mounted flush to the same surface, with the third retro-reflector mounted to a post fixed midway between the other two and jutting at a right angle from the surface. For redundancy, two additional retro-reflectors are mounted on the surface on a line at right angles to the line containing the first two retro-reflectors, and equally spaced on either side of the post. (Figure 1) The target vehicle will contain a large target for initial acquisition and several smaller targets for close range.

There are other target configurations which might provide information on range and orientation [for example see Ref. 1, or see the cross-ratio of projective geometry, Ref. 2].

Geometric Model of the Imaging System

For the purpose of analysis, the lens of the camera is modelled as a pinhole. In a pinhole camera, every object is in focus, regardless of its distance from the camera. For actual lenses, only objects at a given distance, determined by the lens equation, are in perfect focus. Points at other distances from the camera are imaged as "blur circles" whose diameters are proportional to the distance of the point from the ideal distance and to the lens diameter while inversely proportional to the focal length of the lens. The target detection system being developed, however, uses the centroids of detected images. In a statistical sense, the centroid of such an image should be the same whether or not it is in perfect focus. Thus, for purposes of geometrical analysis, the pinhole model is adequate.

While the image plane lies behind the lens at a distance f equal to the focal length of the lens, an imaginary *projected* image plane may lie at any distance behind or in front of the lens. For ease of illustration, a projected image plane is frequently used. We will use a projected image plane lying a distance f in *front* of the lens (Figure 2). A right-handed xyz coordinate system is used, with the positive x -axis extending from C through the center of the projected image plane, and with the positive y and z -axes extending vertically upward and horizontally to the right, respectively.

Determination of Target Range

In Figure 3, C denotes the geometrical center of the lens, P'_1, P'_2 , and P'_3 represent the retro-reflectors in the target, and P_1, P_2 , and P_3 represent the respective images in the image plane. The symbols $\bar{P}_1, \bar{P}_2, \bar{P}_3, \bar{P}'_1, \bar{P}'_2$, and \bar{P}'_3 represent the vectors from C to the respective points on the target and on the image plane. The vector components of \bar{P}_1, \bar{P}_2 , and \bar{P}_3 are, respectively, $\langle f, a_1, b_1 \rangle, \langle f, a_2, b_2 \rangle$, and $\langle f, a_3, b_3 \rangle$. The magnitudes of the vectors \bar{P}'_1, \bar{P}'_2 , and \bar{P}'_3 , representing the distances to the retro-reflectors, are r_1, r_2 , and r_3 , respectively. The fixed distance from retro-reflector 1 (on the center post) to retro-reflectors 2 and 3 is D . The fixed distance between retro-reflectors 2 and 3 is L . The height of the center post is H . The angle between vectors \bar{P}_1 and \bar{P}_2 is θ_{12} . The angle between vectors \bar{P}_1 and \bar{P}_3 is θ_{13} . The angle between vectors \bar{P}_2 and \bar{P}_3 is θ_{23} .

The coordinates of \bar{P}_1, \bar{P}_2 , and \bar{P}_3 are determined directly from the output of the imaging system. The angles θ_{12}, θ_{13} , and θ_{23} are determined by the relations

$$\cos\theta_{12} = \frac{\bar{P}_1 \cdot \bar{P}_2}{\|\bar{P}_1\| \|\bar{P}_2\|}$$

$$\cos\theta_{13} = \frac{\bar{P}_1 \cdot \bar{P}_3}{\|\bar{P}_1\| \|\bar{P}_3\|}$$

$$\cos\theta_{23} = \frac{\bar{\mathbf{P}}_2 \cdot \bar{\mathbf{P}}_3}{\|\bar{\mathbf{P}}_2\| \|\bar{\mathbf{P}}_3\|}$$

Using the Law of Cosines, it is seen that

$$\begin{aligned} r_1^2 + r_2^2 - 2r_1r_2 \cos\theta_{12} &= D^2 \\ r_1^2 + r_3^2 - 2r_1r_3 \cos\theta_{13} &= D^2 \\ r_2^2 + r_3^2 - 2r_2r_3 \cos\theta_{23} &= L^2 \end{aligned}$$

In general, a set of three quadratic equations in three variables can have as many as eight distinct solutions. In this case, however, there are at most four solutions where all values of the variables are positive, since, if (r_1, r_2, r_3) is a solution, then so is $(-r_1, -r_2, -r_3)$. In point of fact, there are never more than three distinct all positive solutions. Three solutions occur when $\theta_{12} = \theta_{13}$. If $\theta_{12} \neq \theta_{13}$, then there are only two distinct solutions in which all three variables are positive. In either case, only one of the solutions has the reflector on the center post pointed toward the camera. The other solutions represent situations where the center post points away from the camera. Since such a target orientation would be undetectable, such a solution may be discarded.

In fact, the method of solution used by Marshall Space Flight Center avoids the necessity of computing all solutions and then rejecting some. It is assumed that the image of the point halfway between P'_1 and P'_3 (the base of the center reflector post) would lie at the point halfway between the images of those points in the image plane. While this assumption is not true, it is a good approximation in the case of the correct solution, and a bad approximation for the spurious solutions. Using an iterative routine (the Newton-Rafson method), the initial guess is improved upon until the system converges to the correct solution. The iterative routine also computes the pitch, roll and yaw of the target. This information, along with the range to the target, is updated and the corresponding rates of change are computed. All range, orientation and rate of change information is then passed along to the guidance routines so that necessary course corrections can be computed for the docking maneuver.

Alternate Solution Method

While the method described above is sufficient, the following method is presented for possible comparison of speed or accuracy.

Assuming that $\theta_{12} \geq \theta_{13}$, Figure 4 represents the target geometry relative to the camera, with C representing the camera, and $P'_1, P'_2,$ and P'_3 representing the three retro-reflectors on the target. The segment P'_1A is perpendicular to CP'_2 . The segment P'_2D is perpendicular to CP'_3 . The segment P'_3B is perpendicular to CP'_1 . Then

$CP'_2 = CA + P'_2A$. Likewise, $CP'_3 = CD + DP'_3$, and $CP'_1 = CB - P'_1B$. Using right triangle trigonometry, and using D and L as defined in the previous section, these three equations may be rewritten as follows:

$$r_2 = r_1 \cos\theta_{12} + \sqrt{D^2 - r_1^2 \sin^2 \theta_{12}}$$

$$r_3 = r_2 \cos\theta_{23} + \sqrt{L^2 - r_2^2 \sin^2 \theta_{23}}$$

$$r_1 = r_3 \cos\theta_{13} - \sqrt{D^2 - r_3^2 \sin^2 \theta_{13}}$$

To solve for r_1 , r_2 , and r_3 , one makes an initial guess that $r_1 = (L/2) \cot(\theta_{23}/2)$, then iterates the equations. If $\theta_{12} < \theta_{13}$, then the 2s and 3s in the above equations should be reversed.

References

1. "Marking parts to aid robot vision", J. W. Bales and L. K. Barker, NASA Technical Paper 1819, NASA-Langley Research Center 1981
2. Geometric Computation for Machine Vision, K. Kanatani, Clarendon Press, 1993

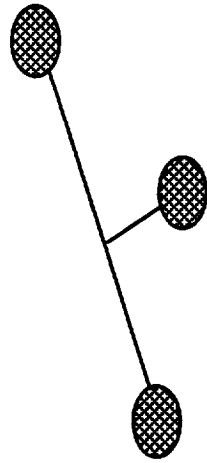


Figure 1: Three-reflecter target configuration

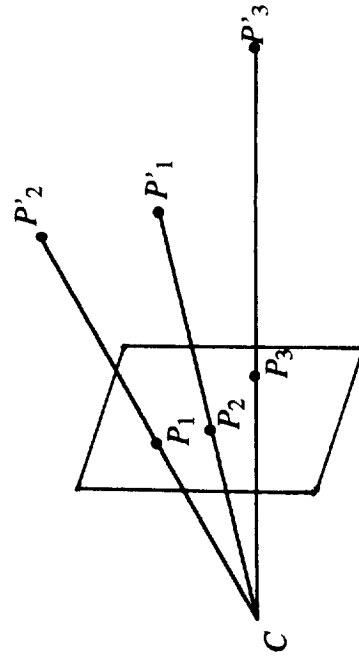


Figure 3: Projection of target onto image plane

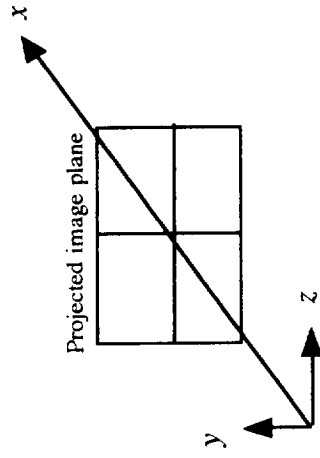


Figure 2: Camera Coordinate System

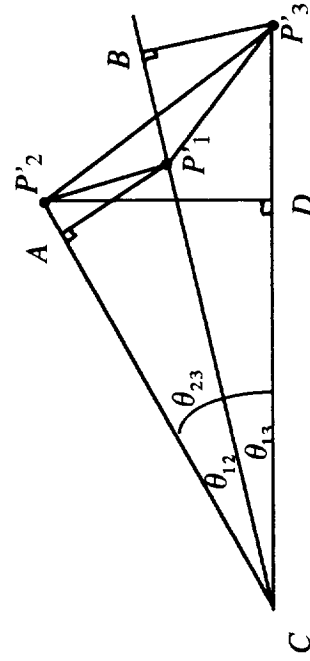


Figure 4: Target geometry for range solution

